Journal of Hydrology 434–435 (2012) 69–77

Contents lists available at SciVerse ScienceDirect

Journal of Hydrology

journal homepage: www.elsevier.com/locate/jhydrol

Using Pacific Ocean climatic variability to improve hydrologic reconstructions

SallyRose Anderson [a,*], Oubeid Aziz [a], Glenn Tootle [a], Henri Grissino-Mayer [b], Anthony Barnett [c]

[a] University of Tennessee, Department of Civil and Environmental Engineering, 67 Perkins Hall, Knoxville, TN 37996, USA
[b] University of Tennessee, Department of Geography, 417 Burchfiel Geography Building, Knoxville, TN 37996, USA
[c] University of Wyoming, Department of Civil and Architectural Engineering, 1000 E. University Ave., Laramie, WY 82071, USA

ARTICLE INFO

Article history:
Received 16 September 2011
Received in revised form 9 February 2012
Accepted 17 February 2012
Available online 25 February 2012
This manuscript was handled by Philippe Baveye, Editor-in-Chief, with the assistance of Noah Knowles, Associate Editor

Keywords:
Snowpack
Reconstruction
Ocean variability
SVD
Climate
Colorado River Basin

SUMMARY

Reconstructions of hydrologic variables are commonly created using tree-ring chronologies. Incorporating climate signals and regionally specific sea surface temperature (SST) indices can greatly improve reconstructive skill. This study performed several reconstructions in the Upper Green River Basin (UGRB), located in the northern portion of the Upper Colorado River Basin. Reconstructed snowpack (April 1st snow water equivalent (SWE)) for the UGRB will provide information on the long-term variability of snowpack and assist in determining the effectiveness of current weather modification efforts. Previous attempts to reconstruct regional snowpack in the UGRB were unsuccessful due to a limited number of tree-ring chronologies. This study increased the number of stations used to represent regional SWE and expanded the spatial area of the study. This resulted in the first reconstruction of UGRB SWE using tree-ring chronologies (R^2 = 0.34). Next, the predictor variable pool is increased by adding climate signals (Southern Oscillation Index (SOI), Pacific Decadal Oscillation (PDO)) and Pacific Ocean SSTs from regions that were determined to be teleconnected with UGRB SWE. Singular value decomposition (SVD) was performed on Pacific Ocean SSTs and UGRB SWE to identify coupled regions of climate (SSTs) and hydrology (SWE). Stepwise linear regression was used to identify the best predictor combinations. Including climate data (SOI) in the model improved the R^2 value from 0.34 to 0.57. The addition of Pacific Ocean SST data further improved the skill of the model (R^2 = 0.63). Reconstructions using Pacific Ocean SST data identified by SVD and climate signals explained a higher degree of SWE variance than reconstructions using tree-ring chronologies and climate data, indicating that Pacific Ocean SSTs and climate signals are useful predictors for snowpack reconstruction in the UGRB. This methodology is transferable to other regions.
Published by Elsevier B.V.

1. Introduction

Tree-ring chronologies are key predictors in reconstructions of hydrologic variables. Tree-ring chronologies have been used throughout the world to develop information about historic climate because ring widths can provide an annual record of temperature and moisture conditions for a region. This study demonstrates the value that climate signals and sea surface temperatures can bring to dendrohydrological reconstructions. To accomplish this, a reconstruction is performed using only tree-ring chronologies as predictor variables. The predictor pool is then augmented with climate signals and sea surface temperatures and another reconstruction is developed. The two results are compared to determine whether there is an improvement in reconstruction skill.

This study focused on the Green River (Wyoming and Utah), located in the Upper Colorado River Basin (UCRB) and the largest tributary to the Colorado River (Fig. 1). Snowpack in the UCRB serves as a natural reservoir, storing water during the winter and releasing it during the spring and summer snowmelt seasons, comprising 50–80% of the annual streamflow (Natural Resources Conservation Service, 2011). In 2005, the State of Wyoming implemented a Weather Modification Pilot Project where ground-based generators released silver iodide into the atmosphere to increase snowpack. A target area for this program was the Wind River Range, the eastern boundary of the Upper Green River Basin (UGRB) and the northern portion of the UCRB. The National Center for Atmospheric Research (NCAR) will evaluate potential increases in snowpack associated with weather modification (Wyoming Weather Modification Pilot Program, 2011). Snowpack measurements for the UCRB, however, date back only to the mid-1900s, restricting the assessment of long-term variability of snowpack in the region.

The first reconstruction study of the UGRB achieved reconstruction models that explained 40% of the variance in streamflow (Stockton and Jacoby, 1976). Woodhouse (2006) continued this research and created a reconstruction model for a streamflow gage on the Green River with an explained variance of 48%. The reconstruction relied heavily on tree-ring chronologies located in northern Colorado and Utah because of the limited availability of

* Corresponding author. Tel.: +1 303 489 2175.
E-mail address: sallyrose.anderson@gmail.com (S. Anderson).

0022-1694/$ - see front matter Published by Elsevier B.V.
doi:10.1016/j.jhydrol.2012.02.037

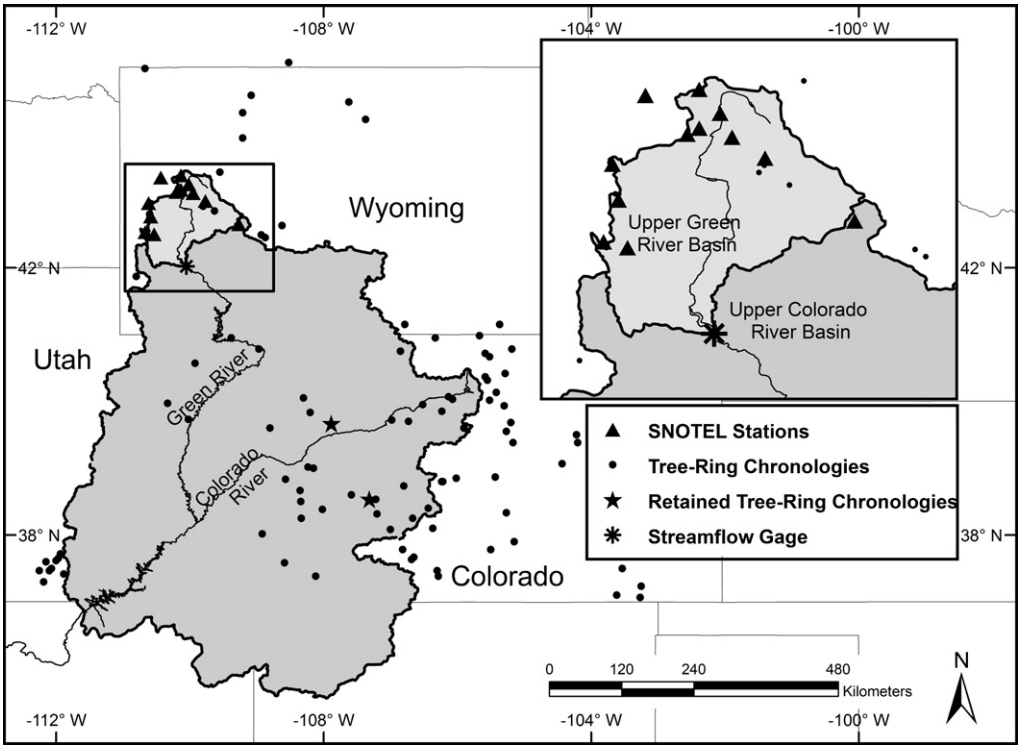

Fig. 1. Location map location map showing the Upper Green River Basin, SNOTEL stations, tree-ring chronologies, and USGS streamflow gage #09211200.

updated tree-ring chronologies in Wyoming (Woodhouse, 2006). Watson et al. (2009) later developed six new chronologies in the foothills of the Wind River Range. These new chronologies allowed Watson et al. (2009) to reconstruct streamflow at multiple headwater gages on the Wind River with explained variances ranging from 40% to 64%. Barnett et al. (2010) were subsequently able to reconstruct streamflow at nine gage sites in the UGRB by incorporating the six tree-ring chronologies created by Watson et al. (2009).

Woodhouse (2003) examined snowpack in western Colorado. Using tree-ring chronologies as predictor variables, she created a reconstruction model that spanned 431 years and explained 63% of the variance in snowpack. Timilsena and Piechota (2008) reconstructed regionalized snow water equivalent (SWE) for the UCRB. Reconstruction models were created for the eastern, western, and southern UCRB for a 480-year period, with explained variances in SWE of 61%, 44%, and 58%, respectively. The northern region of the UCRB spatially coincides with the UGRB. Reconstruction attempts in this region failed because of limited regional tree-ring chronologies (Timilsena and Piechota, 2008).

Graumlich et al. (2003) used Pacific Ocean climate variability to develop streamflow reconstructions for the Yellowstone River, located immediately north of the UGRB. Graumlich et al. (2003) captured Pacific Ocean climate variability using interdecadal to decadal climate signals (Southern Oscillation Index (SOI), Pacific Decadal Oscillation (PDO)). Results showed that including climate indices increased the variance explained by the regression model from 52% to 59% (Graumlich et al., 2003).

The use of a Pacific Ocean sea surface temperature (SST) region that is teleconnected with SWE may improve reconstruction skill compared to the use of predefined climate indices. Coupled relationships between oceanic SST variability and hydrologic variability have been studied using singular value decomposition (SVD). SVD can identify regions of the ocean that are teleconnected with hydrologic variability (Uvo et al., 1998; Rajagopalan et al., 2000; Shabbar and Skinner, 2004; Tootle et al., 2008; Soukup et al., 2009). Tootle and Piechota (2006) used SVD to determine the relationship between Pacific and Atlantic Ocean SSTs and continental United States (US) streamflow. Aziz et al. (2010) identified relationships between western US snowpack and Pacific Ocean SST variability.

Given the successful streamflow reconstructions in the UGRB (Barnett et al., 2010), the first hypothesis is that the incorporation of the new tree-ring chronologies (Watson et al., 2009) will result in a successful reconstruction of UGRB SWE. The second hypothesis states that incorporation of climate signals will further improve snowpack reconstruction skill in the UGRB. The third hypothesis is that the application of SVD to Pacific Ocean SSTs and UGRB SWE will result in the identification of a teleconnected Pacific Ocean SST region that will improve UGRB snowpack reconstruction skill.

The incorporation of climate variability in the form of Pacific Ocean SSTs builds on previous research efforts in the region. The overarching objective is an improved reconstruction of UGRB snowpack that will assist NCAR in their ongoing evaluation of the weather modification program and the establishment of a process for using oceanic variability to augment hydrologic reconstructions.

2. Data and methods

The datasets used to reconstruct snowpack include data from Snowpack Telemetry stations (SNOTEL stations), tree-ring chronologies, climate indices, and Pacific Ocean SSTs. Several steps were undertaken to ensure the strongest datasets were analyzed.

2.1. SNOTEL stations and principal components analysis

There are currently 822 active SNOTEL stations in the western US (Natural Resources Conservation Service, 2011). Twenty SNOTEL stations were identified in and adjacent to the UGRB. Of these 20 stations, 12 have continuous historical data from 1961 to the

present (Fig. 1, Table 1). SNOTEL data are available from the Natural Resources Conservation Service website. April 1st SWE data were used to represent winter snowpack (Woodhouse, 2003).

Data from the 12 SNOTEL stations were analyzed using principal components analysis (PCA) to determine a specific snowpack region in the UGRB (Woodhouse, 2003; Timilsena and Piechota, 2008). PCA was used to reduce the size of the dataset, while retaining critical information (Richman, 1986; Knapp et al., 2002). Principal components with an eigenvalue greater than 1.0 were retained. Stations identified within each component were averaged to create a regional April 1st SWE for the UGRB (Woodhouse, 2003).

2.2. Tree-ring chronologies, correlation, and stability

Tree-ring chronologies were obtained from three sources: the International Tree-Ring Data Bank (ITRDB) website, recent paleohydrologic studies in the UGRB (Gray et al., 2004a,b, 2007), and recent tree-ring collections in and adjacent to the UGRB (Watson et al., 2009). Data for 99 tree-ring chronologies from four different species of trees was obtained. Of the 99 chronologies, 33 were created from Douglas-firs (*Pseudotsuga menziesii*), 30 from pinyon pines (*Pinus edulis*), 10 from limber pines (*Pinus flexilis*), and 26 from ponderosa pines (*Pinus ponderosa*). These four species have been found to be moisture sensitive (Fritts, 1976). The residual tree-ring chronology type was used (Timilsena and Piechota, 2008) for all 99 chronologies (Fig. 1), the chronology type that more closely retains similar statistical properties of hydrological data (Crockett et al., 2010).

The regional April 1st SWE was correlated with each of the 99 tree-ring chronologies using Pearson's correlation method. Chronologies that were positively and significantly ($p < 0.05$) correlated with SWE were retained (Timilsena and Piechota, 2008). To test for temporal stability between tree-ring and SWE data, correlation coefficients between the chronologies and the regional SWE were calculated for a 20-year moving window (Biondi and Waikul, 2004). Chronologies that were positively correlated with regional SWE at a confidence of 90% or greater for all windows, indicating a temporally stable relationship, were retained.

2.3. Climate indices and oceanic lag

The SOI is the index most commonly associated with climatic variability in western Wyoming (Cayan, 1996; Graumlich et al., 2003). The SOI measures air pressure differences between Tahiti and Darwin, Australia. These pressure fluctuations are more pronounced during El Niño and La Niña events. SOI data from the Climate Research Unit available from the National Oceanic and Atmospheric Administration (NOAA) Earth System Research Laboratory (ESRL) website was used. Monthly data are available from 1866 to 2006. The monthly SOI data were averaged to create an annual SOI. Similar to Graumlich et al. (2003), this study also used the PDO, an interdecadal oscillation that shifts phases every 20–30 years. Annual reconstructed PDO data (1470–1998) (Shen et al., 2006) from the National Climatic Data Center (NCDC) and NOAA Climate Reconstruction website were used. Previous studies have identified a lag between SSTs and the influence on hydrologic variables (Tootle and Piechota, 2006; Shabbar and Skinner, 2004). Climate data from the previous year was used to explain SWE for the following April to adjust for this oceanic lag.

Table 1
Location data for SNOTEL stations.

Name	Latitude	Longitude	Starting year	Elevation
Big Sandy Opening	42.65	−109.27	1961	2768
Blind Bull Summit	42.97	−110.62	1948	2637
East Rim Divide	43.13	−110.20	1936	2417
Elkhart Park	43.00	−109.77	1961	2865
Granite Creek	43.35	−110.43	1930	2063
Gros Ventre Summit	43.38	−110.13	1948	2667
Kendall	43.25	−110.02	1938	2359
Loomis Park	43.17	−110.13	1939	2512
New Fork Lake	43.12	−109.95	1961	2542
Snider Basin	42.50	−110.53	1937	2457
Spring Creek Divide	42.53	−110.67	1948	2743
Triple Peak	42.77	−110.58	1961	2591

2.4. Sea surface temperatures (SSTs)

Several studies have identified variations in Pacific Ocean SSTs as significant driving forces of atmospheric circulation in the western US (Mantua et al., 1997; McCabe and Dettinger, 1999, 2002; Clark et al., 2001; Tootle and Piechota, 2006; Hunter et al., 2006; Aziz et al., 2010). Smith and Reynolds (2002) used instrumental-based data to reconstruct SSTs with a resolution of 2° by 2°. The boundaries used for the Pacific Ocean range from 20° south to 60° north latitude and 120° east to 80° west longitude, creating 2792 individual cells (data points). Their dataset is available from 1854 to the present and is updated monthly by NOAA using the Extended Reconstructed Sea Surface Temperature (ERSST) system and the International Comprehensive Ocean–Atmosphere Data Set (ICOADS) (Smith et al., 2008; NOAA ERSST, 2011). Data were obtained from the National Center of Atmospheric Research (NCAR) Climate Analysis Section website.

Evans et al. (2002) developed a reconstructed SST dataset with a resolution of 5° by 5°. The boundaries used for the Pacific Ocean ranged from 60° south to 65° north latitude and 110° east to 65° west longitude, creating 925 individual cells (data points). There are three portions to this dataset. The first is an instrumental-based reconstruction of Pacific Ocean SSTs (Kaplan et al., 1998). The second is a coral-based reconstruction of SSTs created using thirteen annually averaged coral-derived oxygen isotopes (Evans et al., 2002). The third is a tree-based reconstruction of SSTs created using tree-ring proxy indicators (Evans et al., 2002). The instrumental-based dataset begins in 1856, the coral-based dataset begins in 1800, and the tree-based dataset begins in 1590. All three datasets terminate in 1990. Data were obtained from the National Climatic Data Center (NCDC) and NOAA Climate Reconstruction website.

2.4.1. Singular value decomposition (SVD)

Singular value decomposition (SVD) is a statistical technique used to identify coupled relationships between two spatiotemporal fields (Tootle et al., 2008). SVD isolates important modes of variability when identifying relationships between datasets involving grid point arrays and time series (Bretherton et al., 1992; Wallace et al., 1992). SVD analyzes two data fields to find pairs of spatial patterns that explain the mean-squared temporal covariance between the two fields (Bretherton et al., 1992). When using SVD, the two datasets are detrended to remove cross-correlation. SVD was first used in the field of atmospheric sciences by Prohaska (1976) to determine the relationship between monthly mean surface air temperatures over the US and hemispheric sea level pressure patterns. Subsequent studies have used SVD to identify coupled relationships between hydrologic factors and SSTs (Tootle and Piechota, 2006; Aziz et al., 2010).

In this study, SVD was used to determine relationships between Pacific Ocean SSTs and UGRB SWE. The Smith and Reynolds (2002) SST dataset was selected because it provides a larger overlap in the period of record between SSTs and SWE and because it has a smaller grid size. The Pacific Ocean SSTs and SWE anomalies were standardized and used to create matrices. The time dimension of each matrix must be equivalent, while the spatial component can vary in dimension. The time dimension is the overlapping period of

record between SWE data and available Pacific Ocean SST data (lagged 1 year to SWE). The spatial component is comprised of 12 individual SNOTEL stations for the SWE dataset and 2792 cells for the SST dataset.

A covariance matrix for the two spatiotemporal matrices was created, providing physical information to determine the relationship between Pacific Ocean SST cells and UGRB SWE. SVD of the covariance matrix resulted in two matrices of singular vectors (left and right) and one matrix of singular values. The left singular vector matrix contained Pacific Ocean SST data and the right singular vector matrix contained SWE data. The first column of the Pacific Ocean SST matrix was projected onto the standardized Pacific Ocean SST anomalies matrix, generating the first temporal expansion series (1st TES) for Pacific Ocean SST data. The first column of the SWE matrix was projected onto the standardized SWE anomalies matrix, generating the 1st TES for SWE data. The Pacific Ocean SST 1st TES was correlated with SWE and the SWE 1st TES was correlated with Pacific Ocean SSTs, resulting in heterogeneous correlation values for each SWE station and for each Pacific Ocean SST cell. The correlation of the SWE 1st TES with the Pacific Ocean SST matrix revealed the Pacific Ocean SST region that is teleconnected to UGRB April 1st SWE. The correlation of the Pacific Ocean SST 1st TES with the SWE matrix revealed the UGRB SNOTEL stations that were teleconnected with the identified Pacific Ocean SST region.

An index for the Pacific Ocean SST region was created using all Pacific Ocean SST grid cells that were teleconnected (greater than 95% confidence) with UGRB SWE. SVD is useful in the statistical analysis of two spatiotemporal fields, but there are conditions that must be satisfied for SVD to be used correctly (Newman and Sardeshmukh, 1995). The first three modes must explain a significant amount of the variance of the two fields for SVD to be effective in identifying the coupled variability (Newman and Sardeshmukh, 1995).

2.4.2. Use of proxy-based Pacific Ocean SSTs

The Smith and Reynolds (2002) dataset is limited because it begins in 1860. The three portions of the Evans dataset predate this dataset. The Pacific Ocean SST region identified from the Smith and Reynolds dataset was projected onto a map of the Evans dataset. Grid cells from the Evans dataset indentified within the spatial region established by the Smith and Reynolds dataset were used to form a Pacific Ocean SST index for each of the three portions of the Evans dataset.

2.5. Stepwise linear regression and model validation

Stepwise linear regression (SLR) is a common approach for reconstructing hydrologic variables using tree-ring chronologies (Woodhouse, 2003; Gray et al., 2004a; Barnett et al., 2010). SLR uses a forward selection and backward elimination approach for creating regressions. Following Woodhouse (2006), parameters were set with an alpha-to-enter value of 0.05 and an alpha-to-remove value of 0.10. Forward selection includes predictor variables (tree-ring chronologies, climate indices, Pacific Ocean SST indices) in the model and retaining the predictors that are statistically significant, using a threshold alpha value of 0.05. Backward elimination determines which predictors are not statistically significant, using a threshold alpha value of 0.10. These predictors are rejected from the model. The forward and backward processing of predictors continues until the model has selected the predictors that are the most statistically significant.

SLR was used on three pools of predictor variables. First, the predictor pool contained only the tree-ring chronologies that passed pre-screening. Second, the predictor pool contained the tree-ring chronologies and the climate indices (SOI, PDO). Third, the predictor pool contained the tree-ring chronologies and the identified Pacific Ocean SST indices for the Smith and Reynolds dataset and the three portions of the Evans dataset, processed individually. Predicted R^2 is an indicator of how well the model predicts future responses for new observations. It helps identify overfitting of the model. Predicted R^2 is calculated using drop-one cross-validation where one observation is removed from the model and the remaining observations are used to predict the missing value. This process is repeated for each observation. A predicted R^2 value drastically less than the R^2 value indicates that the regression model generated will not predict future responses based on new observations as well as it fits the existing data.

Additional validation statistics were calculated to determine the statistical skill of each model. The standard error of the regressions (S) is used to measure how accurately the model fits the existing data. The standard error is calculated by measuring the distance between each data point and the regression line and averaging the absolute value of the results. Accurate regressions have small standard errors. The Durbin–Watson (D–W) statistic tests for autocorrelation among residuals generated by a regression model, as significant autocorrelation in the residuals can indicate a model that likely excluded necessary predictors. The D–W statistic can vary between 0 and 4. A value of 2.0 indicates that no autocorrelation is present. The sign-test is a nonparametric procedure that identifies the number of agreements and disagreements between paired samples from the observed and calibrated datasets.

3. Results

3.1. SWE and predictor variables

PCA identified one component with an eigenvalue greater than 1.0. All 12 SNOTEL stations were identified within this component, indicating that the 12 stations are statistically similar on an annual basis. The 12 stations were averaged to form a regional April 1st SWE (Woodhouse, 2003).

Of the 99 tree-ring chronologies tested, 19 were positively correlated with SWE at 95% confidence or greater. Stability testing identified two stable chronologies: Rifle (pinyon pine) and Soap Creek (ponderosa pine) (Fig. 1). These two chronologies were retained. None of the six tree-ring chronologies developed by Watson et al. (2009) passed pre-screening for UGRB snowpack. The new chronologies were not used in these reconstructions and the first hypothesis therefore could not be accepted.

The Rifle and Soap Creek chronologies were within 450 km (280 miles) of the sub-basin and are located within the UCRB. Given the easterly-southeasterly movement of weather systems across the western United States, and the rigorous prescreening used to identify tree-ring chronologies that were responding to climate signals seen in the predictand (SWE), we believe the selected chronologies are accurate representations of the climate experienced by the UGRB. While several chronologies are geographically closer to the SNOTEL sites, these chronologies do not represent the climate signal seen by the SNOTEL stations as well. This can be attributed to the different responsiveness of species to hydrologic conditions, the effects of location site conditions (aspect, slope), and potential masking effects of regional disturbances, such as insects and wildfire, that were not detected during chronology development.

SVD was applied to the Smith and Reynolds SSTs dataset and UGRB SWE. The squared covariance fraction for the first mode showed that 93% of variance was explained, indicating a strong relationship between Pacific Ocean SSTs and UGRB SWE. The second and third modes explained 4% and 1% of variance, respectively. Given the high percentage of variance explained (98%) in the first three modes, SVD was applicable for this research (Newman and Sardeshmukh, 1995).

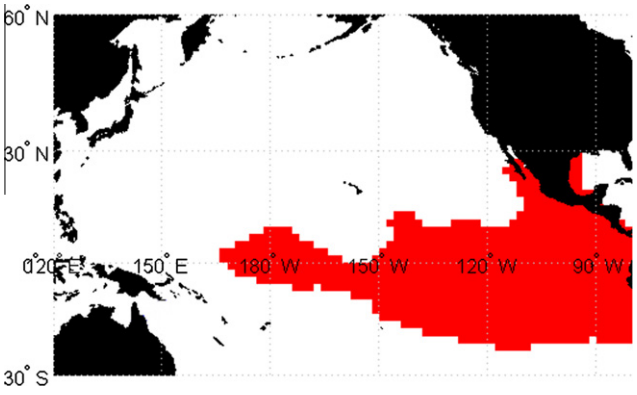

Fig. 2. SST region map identifying the region of the Pacific Ocean that is teleconnected with UGRB SWE.

The Pacific Ocean SST region identified by SVD is defined as 20° south to 15° north latitude and 170° west to 80° west longitude (Fig. 2). All 12 SWE stations were identified as significant. A closer examination revealed the region was located in the equatorial Pacific Ocean and was similar to the Niño 3.4 region, a region used to measure the strength of the El Niño-Southern Oscillation (ENSO) (NCAR, 2011). Previous studies identified ENSO as a climatic driver of snowpack in the UGRB (McCabe and Dettinger, 2002; Hunter et al., 2006).

3.2. Regression models

SLR was performed and six regression models were developed. The first regression model used (only) tree-ring chronologies (TRCs) as predictors. The second regression model used TRCs and climate indices (SOI, PDO). The third regression model used TRCs and the Pacific Ocean SST index developed from the Smith and Reynolds SSTs. The fourth, fifth, and sixth regression models used TRCs and the Pacific Ocean SST indices developed from the three portions of the Evans dataset.

The first regression model explained 34% of the variance and retained the Soap Creek chronology (Tables 2 and 3). The second regression model included climate indices (SOI, PDO). When climate indices (SOI, PDO) were added to the predictor pool, the SOI was retained and the PDO was rejected, indicating the SOI provides the model with information not captured in the tree-ring chronologies. With the addition of the SOI to the model, R^2 improved by 23%, with an explained variance of 57%. Graumlich et al. (2003) found similar results when using the SOI to reconstruct streamflow in the Yellowstone region. In that study, the reconstruction using of tree-ring chronologies resulted in an adjusted R^2 that explained 42% of streamflow variance. The addition of climate signals improved adjusted R^2 by 10% (Graumlich et al., 2003). The improved reconstructive skill of the model that includes climate signals (SOI) is similar in magnitude to the results seen by Graumlich et al. (2003).

Regression models 3–6 included SST indices. SLR retained the SST index in all four models. This shows that regionalized SSTs are useful predictors for reconstructing SWE because they provide the model with hydrologic variability information that is not captured by tree-ring chronologies. Three of the models (models 3, 4, and 5) resulted in an R^2 value that was greater than the R^2 produced using predefined climate indices (SOI). The sixth model used a tree-based SST index and resulted in an R^2 of 45%. While this value is less than the 57% of variance explained by the model using the SOI, it is still an improvement over the first model (tree-ring chronologies). The model using a tree-based SST index extends back to 1590, while the climate signal model is limited by the SOI reconstruction, which dated back to 1866. The regression models that included SST indices explained 45–65% of the variance.

3.3. Statistical and visual analysis

For the six models, the difference between predicted R^2 and the R^2 value is less than 12%, indicating the models were not over-fitted (Table 3). The standard error for each of the six of the regressions is low (Table 3), indicating that all six regression models are statistically valid. The D–W statistics for all six regressions were close to 2.0, suggesting little to no autocorrelation for any of the regressions (Table 3). The sign test for model 1 was significant at $P < 0.05$, while the sign test results for models 2–6 were significant at $P < 0.01$ (Table 3). The graphical results of the six models were examined against the observed values over the calibration period (Fig. 3). No smoothing was performed to allow accurate interpretation of peaks and valleys.

4. Discussion

Barnett et al. (2010) reconstructed annual water-year streamflow for nine unimpaired gages in the UCRB, including USGS gage #09211200. This gage is located on the Green River at the lower boundary of the UGRB (Fig. 1). Given that snowpack provides 50–80% of yearly streamflow in the UGRB (Natural Resources Conservation Service, 2011), a comparison of reconstructed water-year streamflow to the SWE reconstructions may provide insight on which SWE regression model (1 through 6) is most appropriate. R^2 values between observed streamflow and the six reconstructed SWEs (for the calibration period, 1961–1991) ranged from 0.27 to 0.41. The R^2 value between observed streamflow and observed SWE (1961–1991) was 0.50.

Reconstructed streamflow data were obtained from 1615 to 1960 (Barnett et al., 2010). SWE data were reconstructed from 1545 to 1960 (model 1), 1867 to 1960 (model 2), 1861 to 1960 (model 3), 1857 to 1960 (model 4), 1801 to 1960 (model 5), and 1591 to 1960 (model 6). The period examined was determined

Table 2
Regression model component details.

Model	Predictors	Predictors: available/ retained	Retained predictors	Equation
1	TRCs	2/1	Soap Creek (TRC)	4.667 + 0.013670(SOAP CREEK)
2	TRCs, Climate	4/3	Soap Creek (TRC), SOI, Rifle (TRC)	2.596 + 0.007944(SOAP CREEK) + 0.008115(RIFLE) + 3.611(SOI)
3	TRCs, SSTs (S&R)	3/3	Soap Creek (TRC), S&R SST, Rifle (TRC)	222.786 + 0.006507(SOAP CREEK) − 0.08508(S&R) + 0.007993(RIFLE)
4	TRCs, SSTs (Evans-Inst.)	3/2	Soap Creek (TRC), Evans SST (Inst)	6.551 + 0.012457(SOAP) − 7.218(INST)
5	TRCs, SSTs (Evans-Coral)	3/2	Evans SST (Coral), Soap Creek (TRC)	6.661 + 0.012451(SOAP CREEK) − 10.469(CORAL)
6	TRCs, SSTs (Evans-Tree)	3/2	Soap Creek (TRC), Evans SST (Tree)	4.595 + 0.014014(SOAP CREEK) − 7.755(TREE)

Table 3
Performance and validation statistics for SLRs.

Model	Predictors	R^2	Pred. R^2	S	D–W	Sign test (agree/disagree)
1	TRCs	0.34	0.26	4.81	2.24	22/9
2	TRCs, Climate	0.57	0.45	4.06	2.23	26/5
3	TRCs, SSTs (S&R)	0.63	0.52	3.76	2.38	26/5
4	TRCs, SSTs (Evans-Inst.)	0.60	0.52	3.81	2.29	25/6
5	TRCs, SSTs (Evans-Coral)	0.65	0.57	3.58	2.04	27/4
6	TRCs, SSTs (Evans-Tree)	0.45	0.33	4.48	2.38	25/6

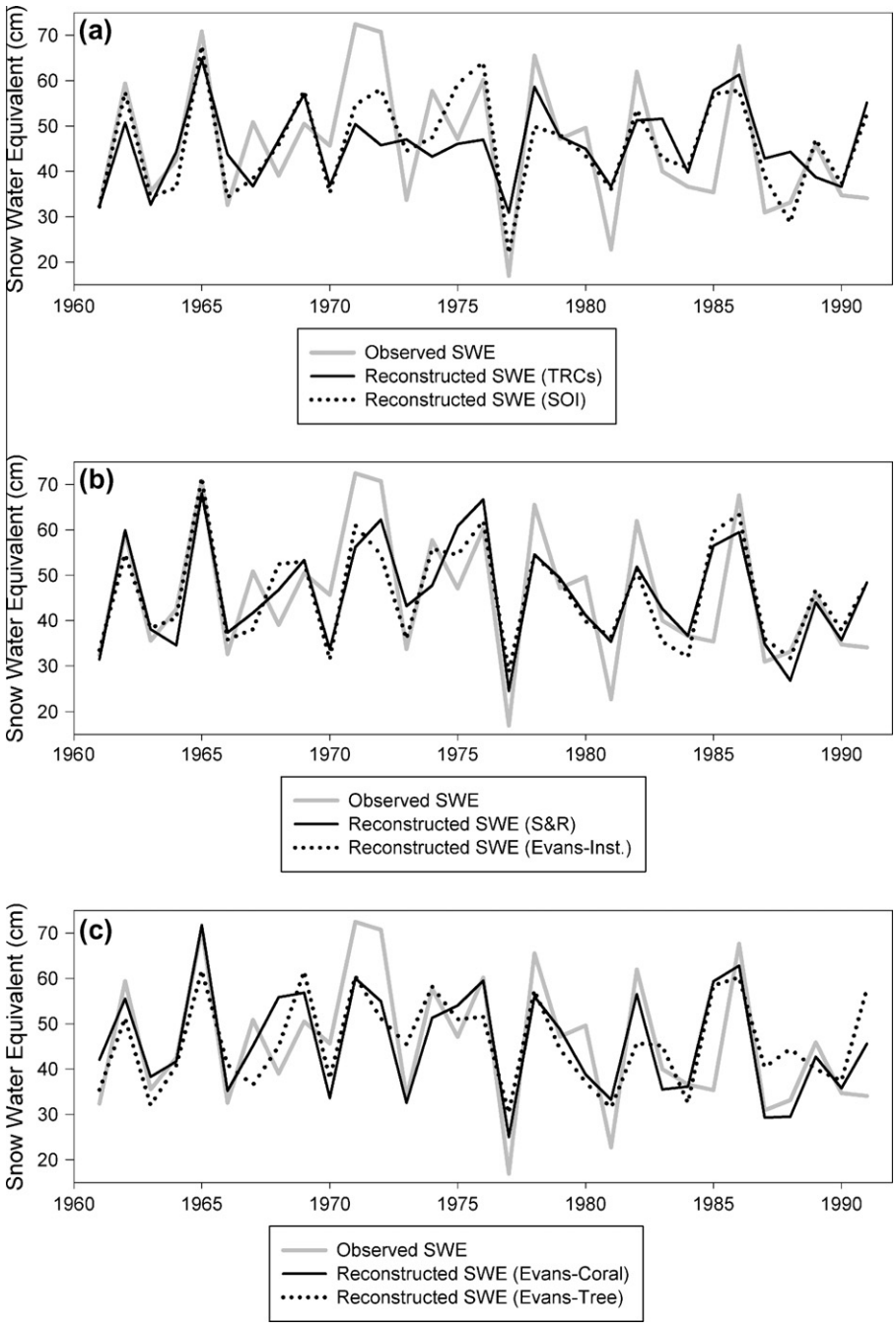

Fig. 3. Calibration period graphical representation of the six regression models over the calibration period: (a) the model using tree-ring chronologies (only) and the model using SOI, (b) models using instrumental-based SSTs (Evans et al., 2002; Smith and Reynolds, 2002), and (c) models using the coral-based and tree-based SSTs (Evans et al., 2002).

by the overlap between the reconstructed streamflow and the reconstructed SWE. The streamflow data and SWE data were standardized (mean of zero, standard deviation of one) and a 25-year (end year) filter was applied (Fig. 4).

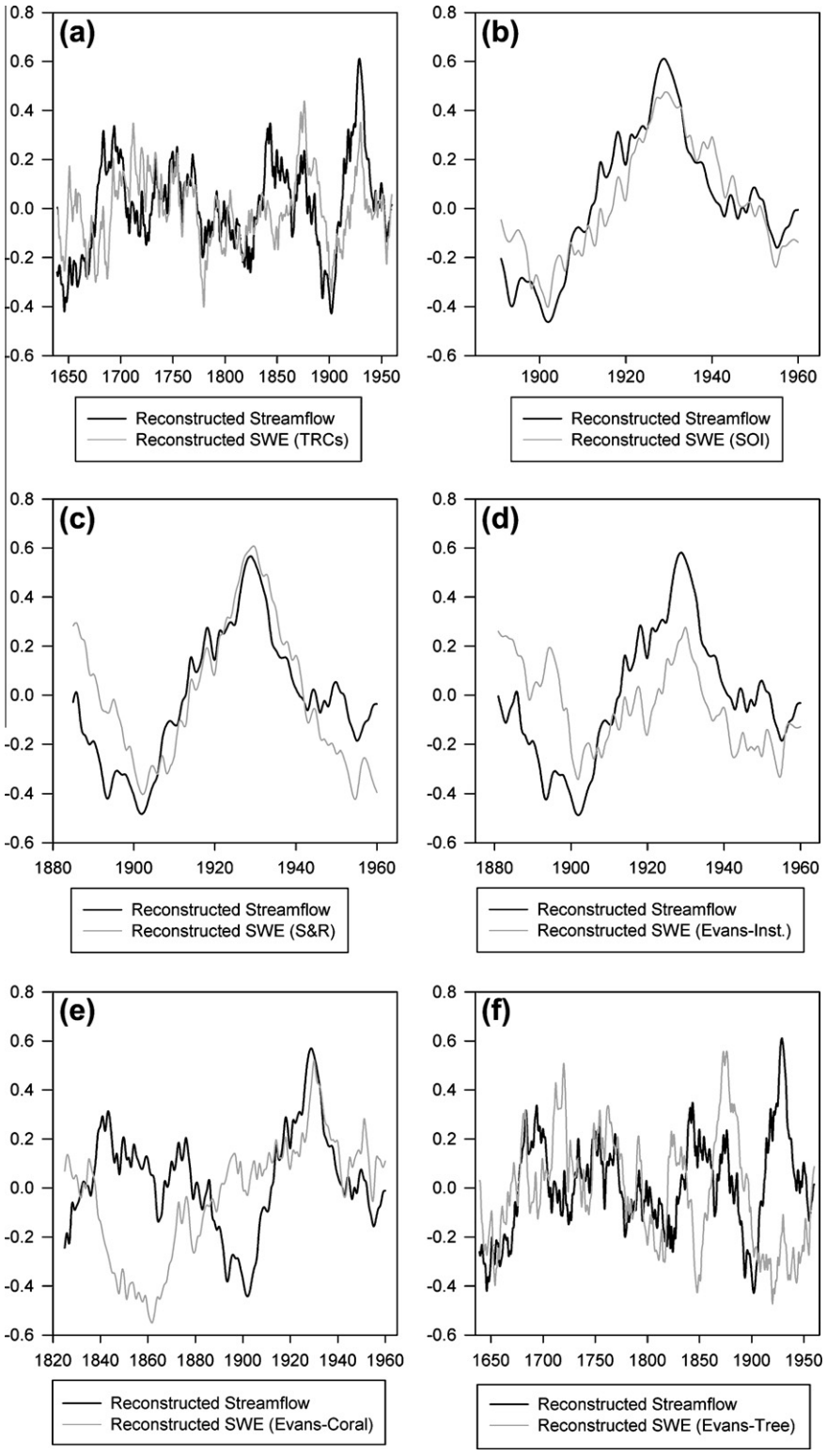

Fig. 4. Reconstructed streamflow and reconstructed SWE graphical representation of standardized reconstructed hydrologic data (streamflow and SWE) over time, with graphs (a)–(f) corresponding to SWE reconstruction models 1–6, respectively.

The second and third models (Fig. 4b and c) align closely with the reconstructed streamflow. The fourth model (Fig. 4d) tends to underestimate the highs and overestimates the lows. While the trends are similar, the extremes exhibited by streamflow are much more pronounced than those captured by the SWE reconstruction. The fifth model (Fig. 4e) reflects the opposite of the trends expressed by streamflow. The sixth model (Fig. 4f) has periods where the two reconstructions are well aligned, but there is opposite trending where the SWE reconstruction is low while the streamflow reconstruction is high, and vice versa. From the visual inspection, the second and third models (SOI and Smith and Reynolds SSTs) are most similar to the reconstructed streamflow. In addition to a visual inspection, streamflow was correlated with SWE for each model. The second and third models (SOI and Smith

and Reynolds SSTs) have R^2 values of 0.34 and 0.40, respectively. These are much higher than the other four models (0.07–0.17). This confirms the results of the visual inspection.

5. Conclusions and future work

This study discovered a stronger correlation between streamflow and the SWE models using the SOI and the Smith and Reynolds SSTs than with other SWE models for the calibration period and the reconstruction period. This validates the second hypothesis. The reconstruction using the Smith and Reynolds SSTs was more highly correlated with regional streamflow data over the reconstruction period than the model using the SOI (0.63–0.59), validating the third hypothesis.

If the UGRB were not an ENSO-influenced region (Graumlich et al., 2003), using the SOI as a predictor variable would not have resulted in improvement of regression model skill. While the incorporation of teleconnected SST regions provided limited improvement over traditional climate signals (SOI) in this study, many regions exist that are not influenced by established climate patterns. The identification of teleconnected SST regions may prove helpful in improving regression model skill when the hydrologic predictand (snowpack, streamflow) is located in a region not influenced by traditional climatic phenomena.

Further research could examine the impact of Atlantic Ocean SSTs on regional reconstructions for a complete representation of oceanic–atmospheric variability. Subsequent research could incorporate North Atlantic Oscillation and Atlantic Multidecadal Oscillation data. Including Atlantic Ocean Oscillations and Atlantic SSTs may result in increased reconstruction skill. Additional studies could use different seasonal components of climate signals in reconstructions. This study used annual SOI and annual PDO. The use of shorter periods (June–December) or winter indices (November–January) may improve reconstruction skill.

Attempts to improve the proxy-based datasets created by Evans et al. (2002) would be beneficial given the length of the reconstructed SST values. While the Smith and Reynolds index provided an increased level of accuracy for the reconstructions, the index limits the reconstruction length because it begins in 1854. The Evans datasets use tree- and coral-based data, which extended the length of the reconstructed SST data and increases the potential length of the reconstruction. Alternatively, the biological data used to create the Evans datasets (tree-ring data, coral isotopes) could be used in a raw form to further enhance the predictor pool.

Investigation into past climatic and hydrologic variability can provide important insights into future water availability. This study skillfully reconstructed UGRB snowpack and developed a greater understand of the linkages between SSTs and regional climatic change. A heightened understanding of past hydrological variability in the UGRB will provide insight into future adaptation and sustainability of the basin and is critical for the evaluation of recent weather modification efforts in the region.

Acknowledgments

This research is supported by the National Science Foundation P2C2 award AGS-1003393.

References

Aziz, O.A., Tootle, G.A., Gray, S.T., Piechota, T.C., 2010. Identification of Pacific Ocean sea surface temperature influences of Upper Colorado River Basin snowpack. Water Resour. Res. 46, W07536.

Barnett, F.A., Gray, S., Tootle, G., 2010. Upper Green River Basin (United States) Streamflow Reconstructions. Am. Soc. Civil Eng. J. Hydrol. Eng. 15 (7), 567–579.

Biondi, F., Waikul, K., 2004. DENDROCLIM2002: a C++ program for statistical calibration of climate signals in tree-ring chronologies. Comput. Geosci. 30 (3), 303–311.

Bretherton, C.S., Smith, C., Wallace, J.M., 1992. An intercomparison of methods for finding coupled patterns in climate data. J. Clim. 5, 541–560.

Cayan, D.R., 1996. Interannual climate variability and snowpack in the western United States. J. Clim. 9, 928–948.

Clark, M.P., Serreze, M.C., McCabe, G.J., 2001. Historical effects of El Niño and La Niña events on seasonal evolution of the montane snowpack in the Columbia and Colorado River Basins. Water Resour. Res. 37 (3), 741–757.

Crockett, K., Martin, J.B., Grissino-Mayer, H.D., Larson, E.R., Mirti, T., 2010. Assessment of tree rings as a hydrologic record in a humid subtropical environment. J. Am. Water Resour. Assoc. 46 (5), 919–931.

Evans, M.N., Kaplan, A., Cane, M.A., 2002. Pacific sea surface temperature field reconstruction from Coral Delta 180 data using reduced space objective analysis. Paleoceanography 17 (1).

Fritts, H.C., 1976. Tree Rings and Climate. Academic Press.

Graumlich, L., Pisaric, M., Waggoner, L., Littell, J., King, J., 2003. Upper Yellowstone river flow and teleconnections with Pacific basin climate variability during the past three centuries. Clim. Change 59, 245–262.

Gray, S.T., Graumlich, L.J., Betancourt, J.L., Pederson, G.T., 2004a. A tree-ring based reconstruction of the Atlantic Multidecadal Oscillation since 1567 A.D. Geophys. Res. Lett. 31, L12205.

Gray, S.T., Fastie, C., Jackson, S.T., Betancourt, J.L., 2004b. Tree-ring based reconstructions of precipitation in the Bighorn Basin, Wyoming since AD 1260. J. Clim. 17, 3855–3865.

Gray, S.T., Graumlich, L.J., Betancourt, J.L., 2007. Annual precipitation in the Yellowstone National Park region since AD 1173. Quatern. Res. 68 (1), 18–27.

Hunter, T., Tootle, G., Piechota, T., 2006. Oceanic–atmospheric variability and western US snowfall. Geophys. Res. Lett. 33, L13706.

Kaplan, A., Cane, M.A., Kushnir, Y., Clement, A.C., Blementhal, M.B., Rajagopalan, B., 1998. Analyses of global sea surface temperature 1856–1991. J. Geophys. Resour. 103 (18), 567–598.

Knapp, P.A., Grissino-Mayer, H.D., Soule, P.T., 2002. Climate regionalization and the spatio-temporal occurrence of extreme single-year drought events (1500–1998) in the interior Pacific Northwest, USA. Quatern. Res. 58, 226–233.

Mantua, N.J., Hare, S.R., Zhang, Y., Wallace, J.M., Francis, R.C., 1997. A Pacific interdecadal climate oscillation with impacts on salmon production. Bull. Am. Meteorol. Soc. 78, 1069–1079.

McCabe, G.J., Dettinger, M.D., 1999. Decadal variations in the strength of ENSO teleconnections with precipitation in the western United States. Int. J. Climatol. 19 (13), 1399–1410.

McCabe, G.J., Dettinger, M.D., 2002. Primary modes and predictability of year-to-year snowpack variations in the western United States from teleconnections with Pacific Ocean climate. J. Hydrometeorol. 3, 13–25.

Natural Resources Conservation Service, 2011. Water Supply Forecasting: A Short Primer. <http://www.wcc.nrcs.usda.gov/factpub/wsf_primer.html> (Accessed July 2011).

Newman, M., Sardeshmukh, P.D., 1995. A caveat concerning singular value decomposition. J. Clim. 8, 352–360.

Prohaska, J., 1976. A technique for analyzing the linear relationships between two meteorological fields. Mon. Weather Rev. 104, 1345–1353.

Rajagopalan, B., Cook, E., Lall, U., Ray, B.K., 2000. Spatiotemporal variability of ENSO and SST teleconnections to summer drought over the United States during the twentieth century. J. Clim. 13, 4244–4255.

Richman, M.B., 1986. Rotation of principal components (review article). J. Climatol. 6, 293–335.

Shabbar, A., Skinner, W., 2004. Summer drought patterns in Canada and the relationship to global sea surface temperatures. J. Clim. 17, 2866–2880.

Shen, C., Wang, W.C., Gong, W., Hao, Z., 2006. A Pacific Decadal Oscillation record since 1470 AD reconstructed from proxy data of summer rainfall over eastern China. Geophys. Res. Lett. 33, L03702.

Smith, T.M., Reynolds, R.W., Peterson, T.C., Lawrimore, J., 2008. Improvements to NOAA's historical merged land-ocean surface temperature analysis (1880–2006). J. Clim. 21, 2283–2296.

Smith, T.M., Reynolds, R.W., 2002. Improved extended reconstruction of SST (1854–1997). J. Clim. 17, 2466–2477.

Soukup, T., Aziz, O., Tootle, G., Wulff, S., Piechota, T., 2009. Incorporating climate into a long lead-time non-parametric streamflow forecast. J. Hydrol. 368, 131–142.

Stockton, C.W., Jacoby, G.C., 1976. Long-term surface-water supply and streamflow trends in the Upper Colorado River basin based on tree-ring analyses. Lake Powell Res. Project Bull. 18, 1–70.

Timilsena, J., Piechota, T.C., 2008. Regionalization and reconstruction of snow water equivalent in the upper Colorado River Basin. J. Hydrol. 352, 94–106.

Tootle, G.A., Piechota, T.C., 2006. Relationships between Pacific and Atlantic ocean sea surface temperatures and US streamflow variability. Water Resour. Res. 42, W07411.

Tootle, G.A., Piechota, T.C., Gutierrez, F., 2008. The relationships between Pacific and Atlantic ocean sea surface temperatures and Colombian streamflow variability. J. Hydrol. 349 (3–4), 268–276.

Uvo, C.B., Repelli, C.A., Zebiak, S.E., Kushnir, Y., 1998. The relationships between tropical Pacific and Atlantic SST and northeast Brazil monthly precipitation. J. Clim. 11, 551–562.

Wallace, J.M., Smith, C., Bretherton, C.S., 1992. Singular value decomposition of wintertime sea surface temperature and 500-mb height anomalies. J. Clim. 5, 561–576.

Watson, T., Barnett, F.A., Gray, S., Tootle, G., 2009. Reconstructed streamflow for the headwaters of the Wind River, Wyoming USA. J. Am. Water Resour. Assoc. 45 (1), 1–13.
Woodhouse, C.A., 2003. A 431-yr reconstruction of western Colorado snowpack from tree rings. J. Clim. 16, 1551–1561.
Woodhouse, C.A., 2006. Updated streamflow reconstructions for the upper Colorado River basin. Water Resour. Res. 42, W05415.
Wyoming Weather Modification Pilot Project, 2011. <http://www.ral.ucar.edu/projects/wyoming/> (accessed July 2011).

Internet Data Sources

Evans SST Data, 2011. National Climatic Data Center (NCDC). National Oceanic and Atmospheric Administration (NOAA) Climate Reconstruction. <ftp://ftp.ncdc.noaa.gov/pub/data/paleo/coral/east_pacific/sst_evans2002/readme_evans2002.txt> (July 2011).
Reconstructed PDO Data, 2011. National Climatic Data Center (NCDC). National Oceanic and Atmospheric Administration (NOAA) Climate Reconstruction. <ftp://ftp.ncdc.noaa.gov/pub/data/paleo/historical/pacific/pdo-shen2006.txt> (July 2011).
Smith and Reynolds SST Data, 2011. National Center of Atmospheric Research (NCAR). Climate Analysis Section. <http://www.cgd.ucar.edu/cas/guide/Data/smith_ersst.html> (July 2011).
SNOTEL Data, 2011. Natural Resources Conservation Service. <http://www.wcc.nrcs.usda.gov/snow/>. (July 2011).
SOI Data. Climate Research Unit (CRU), 2011. National Oceanic and Atmospheric Administration (NOAA) Earth System Research Laboratory (ESRL). <http://www.esrl.noaa.gov/psd/gcos_wgsp/Timeseries/Data/soi.long.data> (July 2011).
Tree-Ring Chronologies, 2011. International Tree Ring Data Bank (ITRDB). Tree-ring data search. <http://www.ncdc.noaa.gov/paleo/treering.html> (July 2011).